

Laser Interactions with Foam-Foil Layered Targets

J. Limpouch^{1,5}, N. G. Borisenko², N. N. Demchenko², S. Yu. Gus'kov², A. Kasperczuk³,
A. M. Khalenkov², V. N. Kondrashov⁴, E. Krousky⁵, J. Kuba¹, K. Masek⁵, W. Nazarov⁶,
P. Pisarczyk⁷, T. Pisarczyk³, M. Pfeifer⁵, V. B. Rozanov², J. Ullschmied⁸

¹ Czech Technical University, FNSPE, Brehova 7, 115 19 Prague 1, Czech Republic

² P.N. Lebedev Physical Institute of RAS, Leninskyi Ave. 53, 119 991 Moscow, Russia

³ Institute of Plasma Physics and Laser Microfusion, 23 Hery St., 00-908 Warsaw, Poland

⁴ Troitsk Institute of Innovation and Thermonuclear Research, 142 190 Troitsk, Russia

⁵ Institute of Physics, AS CR, Na Slovance 2, 182 21 Prague 8, Czech Republic

⁶ University of St. Andrews, School of Chemistry, St. Andrews, KY16 9ST, Scotland, UK

⁷ Warsaw University of Technology, ICS, 15 Nowowiejska St., Warsaw, Poland

⁸ Institute of Plasma Physics, AS CR, Za Slovankou 3, 182 21 Prague 8, Czech Republic

1. Introduction

Low-density foam layers can be used for improvement of the spherical symmetry of direct-drive inertial fusion by smoothing of laser imprint in a relatively thick, relatively hot low-density outer layer of the target [1,2]. Alternatively, transparent underdense foam may be applied as a dynamic phase plate in order to randomize and partly wash out inhomogeneity patterns inside laser beams [3]. Foams with small cells ($D_p \sim 1 \mu\text{m}$) are investigated here experimentally in addition to previous studies of foams with large cells $D_p > 10 \mu\text{m}$ [4, 5].

2. Experimental setup

PALS iodine laser facility in Prague provided 380 ps (FWHM) pulses at the fundamental frequency ($\lambda_1 = 1.315 \mu\text{m}$) and 320 ps pulses at the third harmonic ($\lambda_3 = 0.439 \mu\text{m}$), laser energy was typically in the range of 100 – 200 J. The laser was incident normally on the target; the target surface was placed out of the best focus and thus typical laser irradiances were varied in the range of $I \approx 10^{14} - 10^{15} \text{ W/cm}^2$.

The foams included (1) fine-structured TMPTA foams [6] with submicron pore diameters, foam thickness of 480 μm and densities of 10 and 20 mg/cm^3 ; (2) fine-structured TAC (cellulose triacetate, $\text{C}_{12}\text{H}_{16}\text{O}_8$) foams [7] with pore diameters in the range of 0.5-3 μm and densities 4.5 and 9 mg/cm^3 ; as well as (3) rougher agar-agar foams ($\text{C}_{12}\text{H}_{18}\text{O}_9$) with semi-closed pores [8] of diameter 30-100 μm with densities 5, 10 and 20 mg/cm^3 . In all cases, an aluminum foil, 2, 5 or 10 μm thick was placed at the rear side of foam targets.

Slit image of plasma X-ray emission was recorded by KENTECH low magnification

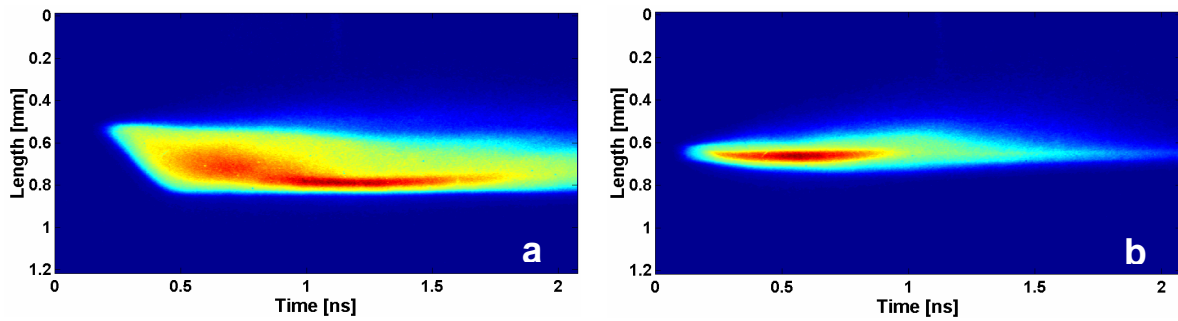


Figure 1: The energy deposition in (a) fine-cell and (b) large-cell foams. *X-ray streak image* of emission from the foam target with Al foil on the rear side. Laser third harmonic pulse is incident from the top down onto the foam surface placed at 500 μm below the best focus (spot diameter $\sim 300 \mu\text{m}$) (a) TAC foam of density 4.5 mg/cm^3 , 380 μm thick with cell diameters 0.5-3 μm , laser energy 168 J. (b) Agar-agar foam of density 5 mg/cm^3 , 380 μm thick with cell diameters 30-100 μm , laser energy 170 J.

x-ray streak camera placed in a side view. The temporal resolution was 70 ps and spatial resolution of 50 μm was in the direction normal to the target surface (target depth). Optical streak camera positioned normally to the target rear side produced time sweep (11 ps/ pixel) of the self-emission from the aluminum foil. Optical diagnostics was carried out by means of 3-frame interferometric system, described in detail in paper [9].

3. Experimental results and discussion

For the laser third harmonic frequency, the utilized foams were mostly underdense (namely, homogenized, fully ionized foam has an electron density n_{eh} less than the critical density n_c). However, the ionized cell walls are overdense, and thus intense radiation cannot penetrate through the cell walls until they are significantly expanded. Cell walls are thinner for foams with fine cells and wall evaporation is then significantly faster. The comparison of X-ray streak images for well underdense foams ($n_{\text{eh}} \approx 0.25 n_c$) with fine and large cells is presented in Fig. 1. For the foam with fine cells, the rear boundary of the heated x-ray emitting area moves fast with the speed of $1.3 \pm 0.1 \times 10^8 \text{ cm/s}$ (error calculated from 4 similar shots) and it reaches the foam's rear boundary during the laser pulse. It is deduced that the position of the first critical surface moves with the above velocity and laser penetrates up this surface. On the other hand, radiation penetration into foam with large cells is limited to about 100 μm (1-3 cell diameters) during the whole laser pulse.

When the density of TAC foam is increased twice, fast propagation of x-ray emitting zone during laser pulse is not observed though foam is still underdense ($n_{\text{eh}} \approx 0.5 n_c$). Minor preheating of the foil at the target rear side is observed at about 0.25 ns after emission from the front side at a typical streak shown in Fig. 2a. Laser is absorbed in the surface layer 30–

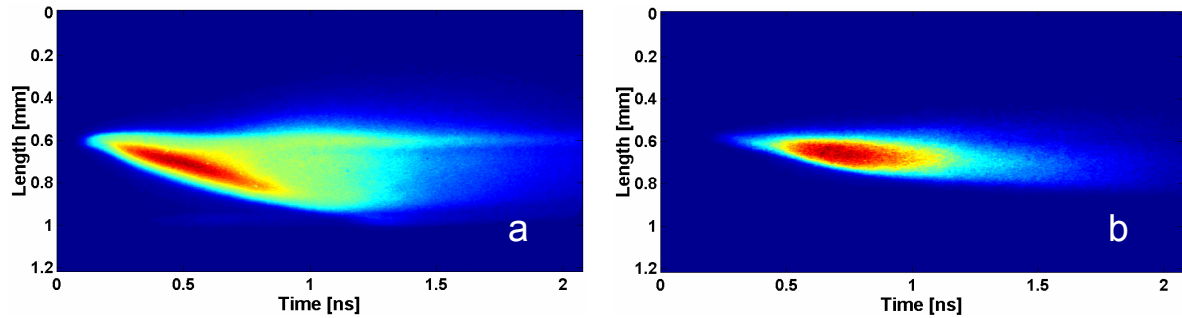


Figure 2: X-ray streak image of emission from a foam target with Al foil on the rear side. Laser is incident from the top down onto the foam surface (spot diameter 300 μm). (a) TAC foam of density 9 mg/cm^3 , 400 μm thick, laser third harmonic, energy 163 J, best focus 500 μm above target. (b) TAC foam of density 4.5 mg/cm^3 , 440 μm thick, basic frequency, energy 163 J, best focus 500 μm below target surface.

–50 μm thick and then thermal wave propagates into the foam with average speed of 3.4×10^7 cm/s and it reaches foil at the target rear side at 1.1 ns after x-ray emission onset. Laser absorption at the foam surface and heat wave propagation is also observed for laser fundamental frequency (Fig. 2b) when even the lightest foam is overdense ($n_{\text{eh}} \approx 2.2 n_{\text{c}}$). Here, the x-ray emission front penetrates only a part of the target.

Optical streak image presented in Fig. 3a was recorded during the same shot as the x-ray streak data in Fig. 2a. Weak optical signal starts before the beginning of the streak at 1.1 ns after the laser pulse. However, comparing Fig. 3a and 2a we conclude that the main optical emission induced by the pressure wave (when it reaches the target's rear side) starts at 2.1 ns after the laser pulse maximum, i.e. approximately 1 ns after the heat wave arrival (Fig. 2a). X-ray streak image cannot follow heat wave propagation inside TMPTA foam due to the target construction. Nevertheless, optical streak in Fig. 3b is fairly similar, the pre-emission starts 0.1 ns before the laser pulse maximum, and the main emission starts with delay of 1.8 ns. This delay is very reproducible for TMPTA foams (variations <10 %). The delay increases with foam density and declines with laser energy.

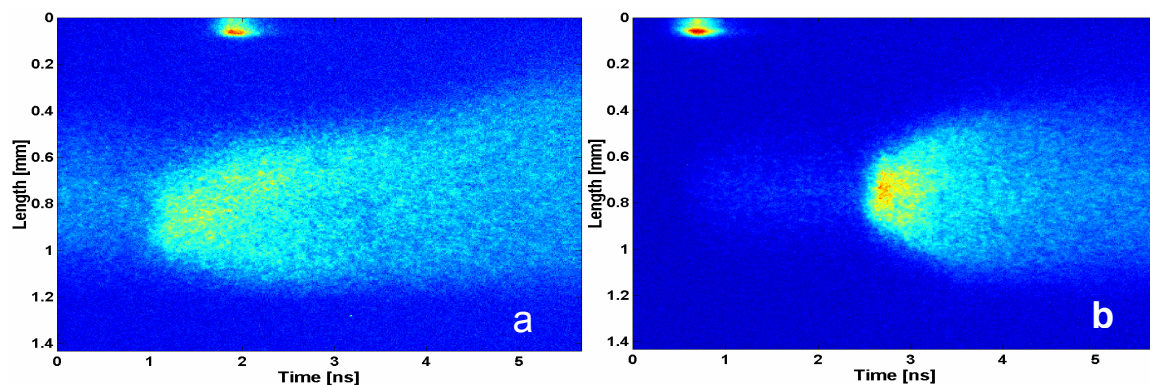


Figure 3: Time history of the optical emission from different foam targets: (a) for the same shot as in Fig. 2a, the centre of fiducial at the figure's top marks time 3 ns after laser pulse (b) for the TMPTA foam of density 10 mg/cm^3 , thickness 480 μm , laser third harmonics, energy 156 J, fiducial marks laser pulse maximum.

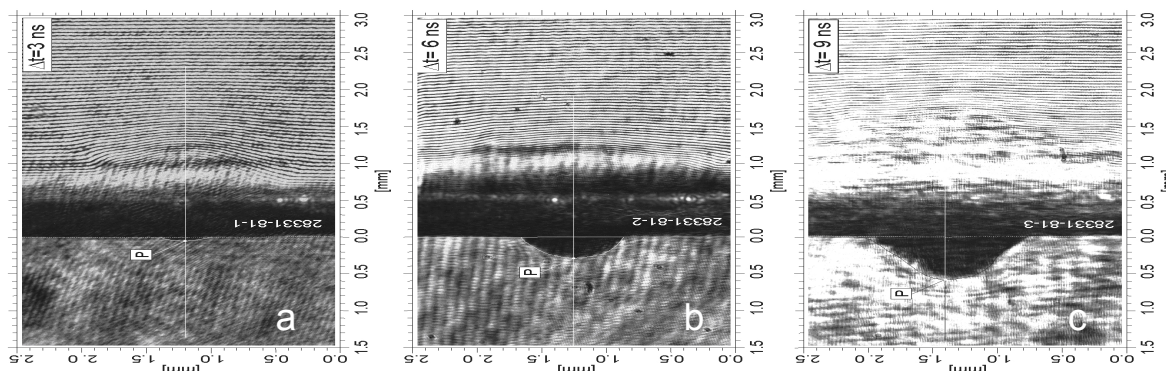


Figure 4: The time resolved shadowgraphy reveals target rear side acceleration (as seen from side) at (a) 3 ns, (b) 6 ns and (c) 9 ns after the laser beam arrival at the target. Laser third harmonics is incident from above on 480 μm thick TMPTA foam of density 10 mg/cm^3 with 10 μm Al foil on the target rear side, laser energy 130 J, and laser best focus 500 μm above the target (laser spot of diameter 300 μm on the target surface).

The motion of the target rear side recorded by three-frame shadowgraphy is presented in Fig. 4. At 3 ns after laser pulse, the motion has just started in the centre of the accelerated region, which is consistent with the start of main emission at optical streak at 2.1 ns. The velocity of the point P between 6 and 9 ns is approximately 9.5×10^6 cm/s; the diameter of the accelerated region is approximately 1 mm at 9 ns after the laser pulse maximum.

4. Conclusions

Interaction of sub-nanosecond intense laser pulses with foams containing fine and large pores has been studied experimentally. It was shown that fast laser propagation is possible only in significantly underdense foams with fine pore structure. Comparison of the experiments with numerical modeling and analytical theory is underway.

Acknowledgements

Support by INTAS project 01-0572 and by project LC528 of CMEYS is acknowledged.

References

- [1] Desselberger M., Jones M.W., Edwards J. *et al.*, *Phys. Rev. Lett.* **68**, 1539 (1992).
- [2] Gus'kov S.Yu., Zmitrenko N.V., Rozanov V.B., *JETP* **81**, 296 (1995).
- [3] Derkach V.N., Bondarenko S.V. *et al.*, *Laser & Particle Beams* **17**, 603 (1999).
- [4] Kalal M., Limpouch J., Krousky E. *et al.*, *Fusion Sci. & Technology* **43**, 275 (2003).
- [5] Limpouch J., Demchenko N.N. *et al.*, *Plasma Phys. Control. Fus.* **46**, 1831 (2004).
- [6] Nazarov W., *Fusion Sci. & Technology* **41**, 193 (2002).
- [7] Borisenko N.G., Akunets A.A. *et al.*, *Laser & Particle Beams* **21**, 505 (2003).
- [8] Bugrov A.E., Burdonskii I.N. *et al.*, *Laser & Particle Beams* **17**, 603 (1999).
- [9] Pisarczyk T., Arendzikowski R. *et al.*, *Laser & Particle Beams* **12**, 549 (1994).